Intent Prediction in pHRI:
Subtask Recognition with Deep Learning

by

Utku Erdem

A Dissertation Submitted to the
Graduate School of Sciences and Engineering
in Partial Fulfillment of the Requirements for
the Degree of

Master of Science

in

Computer Science and Engineering

KOÇ ÜNİVERSİTESİ

January 24, 2020

Intent Prediction in pHRI:
Subtask Recognition with Deep Learning

Koç University
Graduate School of Sciences and Engineering
This is to certify that I have examined this copy of a master's thesis by

Utku Erdem

and have found that it is complete and satisfactory in all respects,
and that any and all revisions required by the final
examining committee have been made.

Committee Members:

Asst. Prof. Dr. Barış Akgün (Advisor)

Prof. Dr. Çağatay Başdoğan (Co-Advisor)

Asst. Prof. Dr. Ayşe Küçükyılmaz

Asst. Prof. Dr. Yıldıray Yıldız

Date:

To my dear grandmother

ABSTRACT

Intent Prediction in pHRI:
Subtask Recognition with Deep Learning
Utku Erdem
Master of Science in Computer Science and Engineering
January 24, 2020

Understanding the human's intention in a physical collaborative task is important for a robot to provide the right type of assistance. We claim that most tasks are made of sequential subtasks and define the human intention as the current desired subtask to be executed. These subtasks have different requirements and a single controller will not be the best way to regulate the interaction. If these subtasks can be recognized in real time, an appropriate controller or controller parameters can be selected. In this work, we propose the idea of subtask recognition, formulate it as a time series classification problem, and develop a deep learning approach to accomplish it. We perform three experiments. The first one ($n = 10$ subjects) verifies the viability of our subtask recognition approach, achieving above 90% test accuracies. The second one ($n = 5$) tests our approach in multiple challenging conditions and shows that it is robust to different human operators, human arm configurations, controller parameters, and environment stiffnesses. The third experiment ($n = 18$) tests our approach in real time. The results provide empirical evidence that the task performance is improved using the proposed approach.

ÖZETÇE

Fiziksel İnsan-Robot Etkileşiminde Niyet Kestirimi:
Derin Öğrenme ile Alt Görev Tanıma
Utku Erdem
Bilgisayar Bilimleri ve Mühendisliği, Yüksek Lisans
24 Ocak 2020

Bir robotun uygun şekilde yardım edebilmesi için, fiziksel işbirliği içeren görevlerde insan niyetinin kavranabilmesi önemlidir. Bu çalışmada, ortaklaşa yürütülen çoğu görevin sıralı alt görevlerden oluştuğunu ve insanın niyetinin yürütülecek olan bu alt görevlere denk geldiğini öne sürüyoruz. Bu alt görevler farklı gereksinimlere sahip olabilirler, dolayısıyla tek bir denetleyici, etkileşimi düzenlemek için en iyi seçenek olmayabilir. Bu alt görevler gerçek zamanlı olarak tanınabildiği zaman, uygun denetleyici veya denetleyici parametreleri seçilebilecektir. Biz, bu çalışmada, alt görevleri tanıma fikrini öneriyor, problemimizi bir zaman serisi sınıflandırması olarak formüle ediyor ve bunu başarmak için derin öğrenme yaklaşımını kullanıyoruz. Bu çalışma kapsamında üç farklı deney gerçekleştirdik. Birinci deneyde ($n = 10$ katılımcı), alt görevleri tanıma yaklaşımımızın uygulanabilir olduğunu ve böyle bir yaklaşımla elde edilen tahmin oranımızın %90'ın üzerinde olduğunu gördük. İkinci deney ($n = 5$ katılımcı) kapsamında yaklaşımımızı çok zorlu koşullarda test ettik ve yaklaşımımızın farklı kullanıcılara, insan kolu konfigürasyonlarına, denetleyici parametrelerine ve çevre katılığına karşı gürbüz olduğunu gösterdik. Üçüncü deneyde ($n = 18$ katılımcı) ise yaklaşımımızı gerçek zamanlı olarak test ettik. Sonuçlar, önerdiğimiz yaklaşım kullanıldığında görev performansının iyileştirilebileceğine dair deneysel bulgular sunmaktadır.

ACKNOWLEDGMENTS

First of all, I would like to thank Asst. Dr. Barış Akgün for accepting to be my advisor. If he did not agree to work with me, I would not be able to meet with robotics, which changed my life entirely. We have been working together for more than two years, and I know he has been thinking about me to make things work better, and I'm grateful for that. I want to admit that I always admire his quick thinking skills and his ability to look at issues from different perspectives. His motivational talks were also inspired me throughout my master's studies. One of the most important lessons that I have learned from him is that his suggestions about concentrating on the big picture rather than minor details. I also want to thank him for his positive attitude and being such an advisor. I hope I will have the honor of working together in my future academic life.

Secondly, I would like to thank my co-advisor, Prof.Dr. Dr. Çağatay Başdoğan. I had the opportunity to learn valuable things from him, but I want to admit that I was mainly trying to learn, especially the way he is presenting the work. He always reminded me to take one step back and question the whole process, which I cannot forget in my future academic life. At the same time, the talks that we had about our study were crucial for this thesis, and it will always remain vivid in my memory.

I would like to thank is Dr. Yusuf Aydın. His knowledge about how to thrive in academic life has always supported me in my graduate years. I would also like to thank him once more for his precious feedbacks and the effort that he put into my study. I will never forget dos and don'ts told by him in my future academic life.

Finally, I would like to thank my dear friends and my family. They always supported me and made me complete this work. I would also like to thank the participants in my work for spending their time on the experiments. Without them, I would not have been able to carry out my experiments and finish my studies.

TABLE OF CONTENTS

LIST OF TABLES

LIST OF FIGURES

ABBREVIATIONS

A_v	performance metric based on amplitude of oscillations in velocity
B	standard admittance controller
b	admittance damping
CPS	controller parameter set
dF_{h}	derivative of the force applied by human
DL	admitance controller based on our deep learning approach
E^{ave}	performance metric based on average effort
EC	experimental condition
F_{h}	force applied by human
F_{int}	interaction force
GT	admittance controller based on ground truth approach
HAC	human arm configuration
m	admittance mass
St	subtask
S/EC	subject-experimental condition combination
v	velocity of the end-effector
v^{ave}	performance metric based on average velocity
v_{ref}	reference velocity

Chapter 1

INTRODUCTION

Physical human-robot interaction (pHRI) and collaboration have the potential to synergistically combine abilities of humans and robots. Humans are good at high-level decision making, error recovery and visual perception while robots are good at low-level control, repetition and precision. A pHRI system can be faster, safer, more efficient, flexible and ergonomic in achieving a desired task. The development of collaborative robot manipulators which are safer and lower cost than their industrial counterparts, and the ubiquity of force/torque (F/T) sensors are bringing us ever closer to practical and widely adopted pHRI.

One challenge in pHRI is understanding the intention of the human so that the robot can best choose how to assist or even take the lead. There are multiple ways to define intention [1]. Most existing works treat human intention in pHRI as a low-level concept such as desire to accelerate or decelerate. We take a high-level and task-based approach. We claim that most pHRI tasks consist of sequential subtasks and define human intention as the current subtask to be executed.

We argue that a single controller parameter set for the robot will not yield the best results for the entirety of a pHRI task. Subtasks have different requirements for quality of interaction and performance, and require different controller parameters or even controllers. For example in a drilling task, (1) the drill needs to be brought close to the intended hole location, (2) the drill needs to be aligned with the surface, and (3) the drilling operation needs to be performed. Each of these *subtasks* have different requirements. In subtask 1, the robot should be *transparent* to the human and move easily. In subtask 2, the robot's motion should be more resistive (damped) to allow precise positioning. In subtask 3, the robot should maintain *stability* by

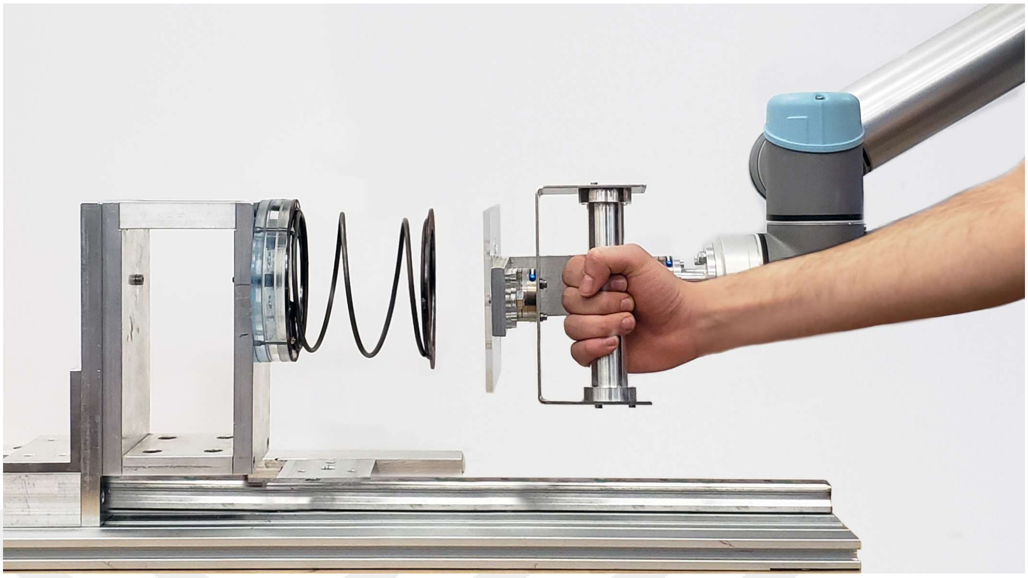

Figure 1.1: Physical human-robot interaction (pHRI).

rejecting disturbances due to contact and drilling. These requirements can be met by selecting different controllers. Meeting all these requirements will increase the task performance.

1.1 Thesis Statement

Typical pHRI task consists of several subtasks. We define human intention as the desired subtask to be executed. These subtasks have different requirements and a single controller will not be the best way to regulate the interaction. When these subtasks can be recognized in real time, an appropriate controller or controller parameters can be selected, so that overall efficiency and task performance can be increased.

1.2 Contribution

First, we divide a typical pHRI task into subtasks and want to show that subtask recognition is viable during the interaction. We formulate subtask recognition in pHRI as a time series classification problem and use deep learning to tackle it. We argue that a machine learning (ML) based approach is better than a rule-based one for multiple reasons. The latter is prone to human error, requires expertise that may not be present at the robot deployment site, may require fine-tuning for different conditions and may be impossible to achieve for complex pHRI tasks. An ML based approach will be more robust given enough data.

We perform an experiment (see Figure 1.1) with 10 participants to show that subtask recognition; (1) is feasible with high recognition rates, and (2) can be generalized between users, i.e., a model trained with one participant can be used to predict the subtasks of others. We then perform another experiment with 5 participants to test our approach in more challenging conditions to (1) verify the results of the first experiment and show that it is robust against changes in (2) human arm configuration (human arm stiffness), (3) controller parameters and (4) environmental stiffness. We perform multiple evaluations (train-test conditions), most of which have recognition rates above 90%, to support our claims. We conduct one last experiment with 18 participants to show that our method can be utilized in real time to improve task performance.

1.3 Outline

The rest of this thesis is organized as follows: Chapter 2 presents the earlier related studies estimating human intention in pHRI systems. The proposed approach for subtask recognition is introduced in Chapter 3. Section 3.1 presents the preliminaries for the human subject experiments. The experimental study investigating the viability of the proposed approach is reported in Chapter 4. The robustness of such an approach against several conditions that can be encountered during a pHRI task is investigated by another experimental study reported in Chapter 5. An implementation of the proposed subtask recognition approach in real time and performance of an adaptive interaction controller utilizing the proposed approach in another experimental study is presented in Chapter 6. A thorough discussion is given in Chapter 7, and conclusions and future research directions are provided in Chapter 8.

Chapter 2

RELATED WORK

Impedance/admittance based interaction controllers [2,3] are widely used to regulate the physical interaction in pHRI systems. A robot can adjust its contribution to comply with the intentions of the human by adapting the parameters of its controllers. Such adaptation requires the prediction of the human intention during interaction through the haptic communication channel between the human and the robot. In this study, as mentioned in the introduction, we define human intention as the current subtask of an overall pHRI task.

Communication between partners in a physical collaborative task is crucial for fluency and efficiency. Humans can do this in a non-verbal way through the haptic channel. For instance, Stefanov et al. [4] propose executor (executes the task) and conductor (guides the task) roles for human-human interactions. They show that intent communication, of which role to take, is possible with the use of haptic cues.

We argue that utilization of machine learning (ML) in the domain of pHRI to detect human intention will perform better compared to rule-based approaches. Within this scope, we present earlier related works in two separate class: ones involving rule-based approaches and others utilizing machine learning.

2.1 Studies Involving Rule-Based Approaches

Although humans can communicate through haptic cues in order to understand each other's intentions [4], robots cannot make use of such cues easily. This is one of the challenges in establishing reliable communication between humans and robots during physical interaction. One approach to solve this is to use force-based information. Mörtl et al. [5] adjust the contribution of the robot dynamically according to human partner's intentions by using the interaction force and its direction through a role exchange mechanism suggested in [6, 7]. Medina et al. [8] propose an arbitration mechanism which dynamically adjusts the contribution of the robot based on forces applied by the human. Here, robot assumes that human partner intends to change the direction of motion when they exceed a predetermined force threshold in that direction. Another approach is to utilize kinematics information. Ikeura and Inooka [9] use velocity of the manipulated object, instead of force based information, to alter the damping parameter of a variable admittance controller. Several other studies utilize both the derivative of force applied by the human and the velocity of the manipulated object to predict whether the human intends to accelerate or decelerate an object [10]. Aydin et al. [11] improve the approach proposed in [10] by adding a fuzzy intention estimator and show its effectiveness in a simulation. Instead of using the derivative of the interaction force, Lecours et al. [12] prefer the acceleration output of the admittance controller directly so that noise in force measurement would not adversely affect the intention estimation. In [10–12], damping is increased (decreased) when the human intention is estimated as deceleration (acceleration). These studies show that force-based (force, F and derivative of the force, dF) and kinematics information (velocity of the object, v) can be used in predicting human intent in pHRI.

Knowledge of human arm stiffness can give hints about the intention as well. Tsumugiwa et al. [13] estimate human arm stiffness but this requires additional computational effort and may not be accurate if the pHRI task is complex. Grafakos et al. [14] propose to use surface EMG to predict whether human intends to perform operation requiring high precision movements or not. They assume that humans tend to co-contract their muscles when they perform such movements while activation levels of muscles is kept low when the operation does not require high precision. Consequently, if a rise in the muscle activation is detected through surface EMG, the damping is altered on-the-fly accordingly to allow fine incremental movements for increased precision. Their approach decreases the energy consumption of the human and increases motion accuracy. However, placing a surface EMG is not always a feasible solution as it requires additional infrastructure. On the contrary, we propose a method which does not require any other investments but uses the utilities of the robots alone.

Common shortcoming of all the aforementioned studies is the exclusive use of rule-based approaches, which means that parameters/rules need to be tuned manually for different tasks or different users.

2.2 Studies Involving Machine Learning

As a more promising choice over the rule-based approaches, ML has the potential to yield more generic and flexible approaches to estimate human intention in pHRI. For instance, Rozo et al. [15] propose a framework for a user to teach collaborative skills to a robot from demonstrations. Robot learns how to adjust its impedance to execute the task during physical collaboration. Dimeas et al. [16] propose a variable admittance controller based on reinforcement learning for human-robot co-manipulation where damping of the controller is regulated to minimize jerk. These approaches do not estimate or use human intention but learn how to execute a task collaboratively with a human to improve the quality of interaction. However, learning each task, or a specific policy for all tasks may not always be feasible. For instance, a task like drilling itself can be inherently jerky, which makes learning a policy to minimize jerky motion could be challenging. Furthermore, minimizing jerk will often not be the only desirable robot assistance. In such cases, predicting human intent will enhance the applicability of the approach.

ML based techniques can also be used for estimating human intent in collaborative tasks involving physical interaction. Such approaches can offer an end-to-end framework, so, estimations of the human intent would be more generic. To this end, there are several studies combining different types of machine learning algorithms with force-based and kinematics information. Townsend et al. [17] utilize a neural network to predict intended human motion based only on the available recent data without any prior estimation or calculation, and provide empirical evidence for the potential of their approach. Evrard et al. [18] develop a role-switching model using the interaction forces and Gaussian Mixture Models. Using this model, robot is able to switch its role from leader to follower or vice versa according to estimated role (i.e. intention) of the human. Wang et al. [19] use interaction forces and a Hidden Markov Model to estimate human impedance and decide whether human intends to actively lead the execution of the task or to comply with the robot's agenda for a handshaking task. Parameters of the admittance controller are selected according to the estimated human intention. Ranatunga et al. [20] develop a system for rehabilitation purposes utilizing neural networks and estimate intended human motion, so that the admittance controller parameters are altered on-the-fly as needed. These approaches show that it is viable to use ML in pHRI but none of them focuses on the idea that a task consists of several sequential subtasks and these can be recognized during execution.

Ikemoto et al. [21] propose a method in which a robot learns when to switch between several successive sets of desired postures to execute an assisted standing-up and walking task, while human imitates a parenting role to teach the robot when to execute the switching. Intermediate desired postures and executing each one successively to stand-up or walk can be considered to be related to our sequential subtask idea but their approach is highly specific to a single robot and a task. Likewise, during the execution of a typical pHRI task, the robot can adapt its behavior (by altering parameters of interaction controller) once the subtask reflecting the human's current intention is identified to increase the performance of the subtask. In this study, we aim to identify these subtasks as the task is being executed.

Chapter 3

APPROACH

We hypothesize that a typical pHRI task consists of several subtasks, and in this study, we first divide a pHRI task into subtasks, then define the human intent as the desired subtask to be executed. Recognizing subtasks during interaction in real time is useful as the robot can adapt its behavior and comply with the human intention. This adaptation can be done by changing controller parameters or switching to a different controller type, for each subtask. In this way, different subtask requirements can be addressed easily to increase overall efficiency and decrease human effort. Our main contribution in this work is the idea of subtask recognition in a real pHRI scenario.

In this study, we aim to show that subtask recognition is viable and robust to the possible changes in the system, and furthermore, utilizing an adaptive approach based on subtask recognition can enhance the task performance during a collaborative task. To demonstrate these, we consider a pHRI task that is composed of salient subtasks. Human applies force to the robot's end-effector to move it along a line while the robot is interacting with the environment to perform a task (e.g. drilling). To regulate the interaction between human and robot, we use an admittance controller depicted in Figure 3.1. The resultant interaction force between the human, the robot and the environment can be measured by a force sensor, filtered with a low-pass filter, and the filtered interaction force, F_{int}, can be fed to the admittance controller. Then, the admittance controller generates the reference velocity, v_{ref}, which is sent to the robot's controller.

In such an interaction, the velocity, v, of the robot's end-effector can be measured by its internal sensors, while force applied by human operator, F_{h}, can be measured with an additional force sensor. As mentioned in Chapter 2, velocity, v, human force, F_{h}, and its derivative, dF_{h} are utilized to predict human intentions during the interaction. These measurements are readily available in most pHRI systems which makes our approach more applicable.

At each time step t, the aforementioned features, $x_t = [F_{\mathrm{h}}(t), dF_{\mathrm{h}}(t), v(t)]$ can be acquired in real time and be used in recognition. However, a single data point may not contain sufficient information to recognize a subtask. Instead, it makes more sense to look at a history of data points, i.e., to work on a time series. Thus, the problem becomes, given a window of data points of size w containing $\{x_{t-w+1}, \ldots, x_t\}$, what is the current subtask, $y \in Y$, where Y is the set of all the subtasks. The behaviors of both the human and the robot is nonlinear, configuration dependent, and time varying [22] which make the interaction complex and nonlinear. Although one can attempt to design a rule-based approach utilizing a window of measurements, it is highly challenging to obtain generic rules to predict human's intent. Additionally, a desirable subtask recognition approach should handle variety of conditions which can be encountered during the execution of a pHRI task:

- Different users can work with the robot.
- Users may get tired or prefer changing their arm configurations, leading to changes in human arm impedance.
- Different control architectures or parameters may be employed for different subtasks.
- Robot can interact with different environments.

In short, an approach to recognize subtasks should capture complex and nonlinear relations in data and be robust to variety of conditions mentioned above. We argue that a ML based approach is suitable to address these challenges more effectively than a rule-based one. In particular, as the data is in the form of a time series, subtask recognition can be formulated as a time series classification problem and one among many appropriate techniques such as Hidden Markov Models, Conditional Random Fields, Convolutional Neural Networks, Recurrent Neural Networks (RNN) etc., can be utilized. In this study, we use a RNN, specifically long short-term memory (LSTM) architecture, for subtask recognition as these are high capacity models capable of learning nonlinear and complex structures in sequences.

3.1 Experimental Setup and Protocol

We collected data by conducting three sets of pHRI experiments. The first experiment focused on verifying the viability of subtask recognition using ML. The second experiment focused on assessing the robustness of the trained models based on the aforementioned requirements. This experiment had multiple different experimental conditions and we trained our models using data of one condition to test with others. In the third experiment, we implemented the model trained with the data of the participants in the first experiment to show that subtasks can be recognized in real time and an adaptive admittance controller based on subtask recognition can improve the task performance during a collaborative pHRI task.

3.1.1 Admittance Controller

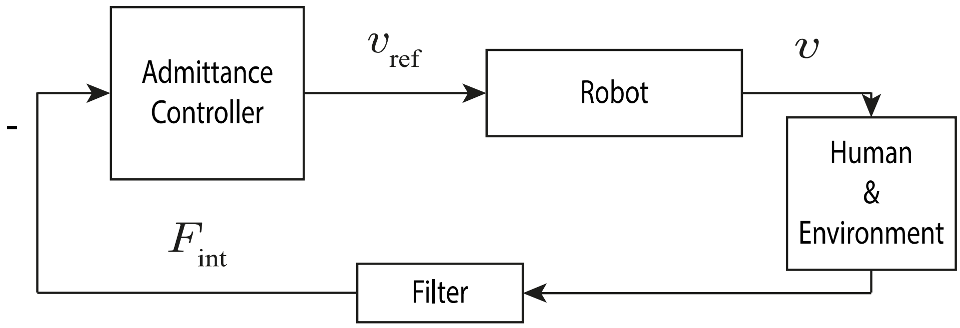

Figure 3.1: Our pHRI control architecture.

An admittance controller architecture is used to regulate the interaction between human and robot (Figure 3.1). Our admittance controller has the form, $v_{\text{ref}}(s)/F_{\text{int}}(s) = 1/(ms + b)$, where m and b stand for the admittance mass and damping parameters, respectively.

During the interaction, subjects apply force to the robot's end-effector while the robot is also interacting with the environment. The resultant interaction force is measured by a force sensor, filtered, and the filtered interaction force, F_{int}, is fed to the admittance controller which generates the reference velocity, v_{ref}, for the robot's internal motion controller.

3.1.2 Experimental Protocol

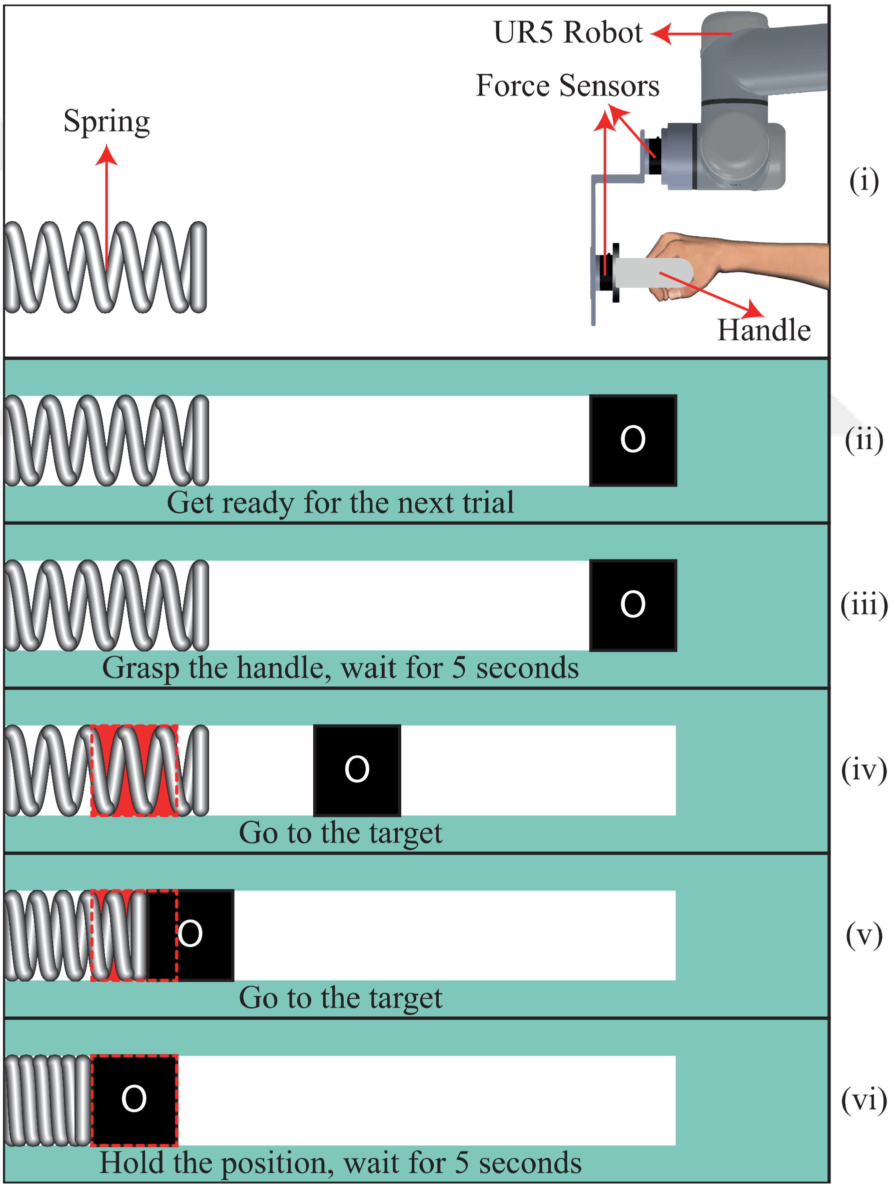

Figure 3.2: Experimental setup and visual feedback given to subjects.

We select our pHRI task to be a one-dimensional (1-D) abstraction of a drilling process. We restrict ourselves to a 1-D task to have more control over the experimental conditions. During both experiments, subjects interact with a UR5 robot (Universal Robots Inc.), as shown in Figure 1.1, to perform the task. The environment is represented by a linear spring where the task is to compress it by a certain amount starting from an initial position. We define 5 subtasks for this task. These are in the execution order, idle robot state, grasping the robot handle, moving towards the spring, making contact with the spring and compressing, and holding the compressed spring. During the experiments, subjects can track the robot's current position and the target location on the screen as a visual feedback (Figure 3.2). The black rectangle labelled as 'O' represents the position of the end-effector. The red rectangle represents the target location. The details of the subtasks are as follows:

St1 Idle: Each trial begins with this subtask where subjects were asked not to touch the robot handle until the prompt "Get ready for the next trial" disappears from the screen (Figure 3.2-ii). We considered this subtask to be able to differentiate whether there the human is present or not.

St2 Holding the handle: Following St1, a prompt, "Grasp the handle, wait for 5 seconds", was displayed on the screen (Figure 3.2-iii). Subjects were asked to maintain the current position. The aim is to collect data when the human grasps the handle to signal the beginning of the task.

St3 Free movement: After St2, a target was shown along with the prompt, "Go to the target" (Figure 3.2-iv) on the screen. To move to the target, the spring representing the environment must be compressed. To achieve this, the human must approach the spring first to make contact. We take this subtask to be the free movement after St2 and right before contact. Thus, St3 is similar to a case where the robot is guided by the human to approach a surface to operate on.

St4 Contact: As soon as St3 ends, contact with environment (i.e. contact subtask) begins and this subtask continues till target is reached (Figure 3.2-v). Stabilizing a contact with environment is challenging in pHRI [23, 24]. Moreover, compressing a spring (similarly, pushing a drill to penetrate into a surface) requires significant effort by the human. Thus, we argue that this should be a separate subtask.

St5 Hold: When the subject reaches to the target location, the prompt "Hold the position, wait for 5 seconds" appears (Figure 3.2-vi). This subtask simulates the case when the users will drill the surface up to a point and maintain this position some time to finalize the desired clearance.

Durations of St1, St2, and St5 were selected to make them comparable. In St3, as each participant was free to move with a speed of her/his desire, we could not foresee the duration of motion. However, due to the nature of St4, duration of St4 is shorter than that of other subtasks.

We would like to mention that it may not be easy to define a boundary between St4 and St5 due to the nature of contact interactions. However, it is possible to separate them as well as others in a pHRI task similar to ours. Note that our task consists of the subtasks mentioned above such that these subtasks can be separated by expert supervision based on position information alone.

In each trial, subjects were asked to maintain their given arm configurations. In each experiment, we used several sets of admittance controller parameters since different controller parameters can be utilized during the execution of a general pHRI task. The values of these parameters (see Table 3.1) were chosen considering the stability maps provided by Aydin et al. [24]. During the experiments, subjects were given a training session before data collection to familiarize themselves with the experimental setup. Each subject performed back and forth motions as training.

Compliance with Ethical Standards

Ethical approval: The experimental study was approved by the Ethical Committee for Human Participants of Koc University.

Informed consent: In this study, all the subjects gave informed consent about their participation in the experiment.

3.1.3 Data Collection and Preprocessing

We recorded human force, F_{h}, using a force sensor and the end-effector velocity, v, from the internal sensors of the robot, both at a rate of 125 Hz. F_{h} was filtered using a low-pass filter, and its derivative, dF_{h}, was calculated using the forward difference method at each time step. Then, the data was averaged using a sliding window of size 6. Finally, the data was z-normalized before being input to learning.

3.1.4 Deep Learning Setup

As mentioned in Chapter 3, our machine learning model is a LSTM model with a softmax output later. The input is a window of sequential normalized data of length ω and the output is the corresponding subtask. To decide on the architecture parameters, we swept for number of recurrent layers, hidden layer size, and the window size over the sets of {1, 2}, {2^1, 2^2, ..., 2^{10}}, {5, 10}, respectively, using the data collected from the first experiment (Section 4.2). Adam weight update rule with a learning rate of 0.001, mini-batch size of 32 and a dropout rate of 0.2 before the output layer to prevent overfitting were used in training of all the models. The best parameter set was $\{2, 2^{10}, 5\}$ with 96.7 (0.9)% (mean (standard deviation)%) accuracy. However, this came at the expense of considerable computational burden during training. Furthermore, accuracy gains were not significant for the more complex models. We accepted test accuracies over 90% and decided to use the parameter set $\{1, 2^6, 5\}$ which resulted in 91.7 (2.2)% average accuracy to reduce the computational effort. All the LSTM models trained and reported in this thesis use these hyperparameters.

3.1.5 Experimental Conditions

We used three different springs having stiffness values of K_{low}, K_{nom}, and K_{high}, two different sets of controller parameters (CPS1 and CPS2), and two different human

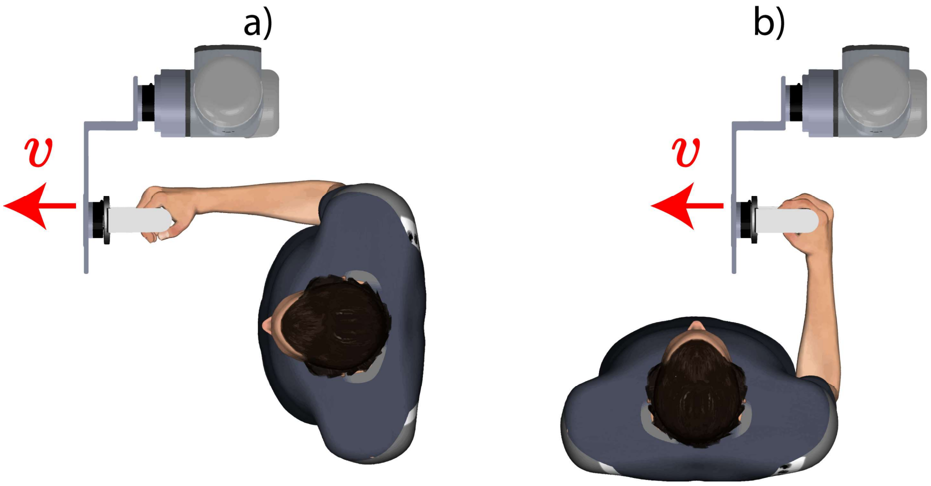

Figure 3.3: Two different human arm configurations.

arm configurations (HAC1 and HAC2) (see Table 3.1 for details). We conducted the first experiment with EC1. Experimental conditions other than EC1 were devised after obtaining promising test scores from the first experiment. They were chosen to investigate the robustness of our approach, based on the situations that are likely to be encountered during physical human-robot collaboration.

Table 3.1: Experimental Conditions

	Stiffness (N/m)	Human Arm Config.	Controller Para. Sets, m [kg], b [Ns/m]
EC1	$K_{nom} = 1000$	HAC1 (Figure 3.3a)	CPS1: $m \in \{5, 10\}$, $b \in \{50, 125, 200\}$
EC2	$K_{low} = 700$	HAC1 (Figure 3.3a)	CPS1: $m \in \{5, 10\}$, $b \in \{50, 125, 200\}$
EC3	$K_{high} = 1670$	HAC1 (Figure 3.3a)	CPS1: $m \in \{5, 10\}$, $b \in \{50, 125, 200\}$
EC4	$K_{nom} = 1000$	HAC2 (Figure 3.3b)	CPS1: $m \in \{5, 10\}$, $b \in \{50, 125, 200\}$
EC5	$K_{nom} = 1000$	HAC1 (Figure 3.3a)	CPS2: $m \in \{5, 10\}$, $b \in \{20, 160, 300\}$

Chapter 4

EXPERIMENT-I: VERIFICATION

The first experiment is designed to check whether the subtask recognition concept is viable or not. This experiment was conducted with EC1 (see Table 3.1). The purpose is to collect more data on a narrower range of conditions to investigate subtask recognition in detail and as such, only the controller parameters were varied. This experiment was completed with 10 participants (9 male, median age: 30).

This experiment consists of 6 (2x3) different controller parameter combinations (CPS1). During the training phase, each participant performed backward-forward motions twice with each combination to familiarize themselves with the setup. During the actual data collection phase, each participant did the task 5 times with all the combinations, resulting in 30 (5x6) trials per participant for a total of 300 trials. An example evolution of each feature (i.e., v, F_h, dF_h) with respect to time is shown in Figure 4.1 for a single subject.

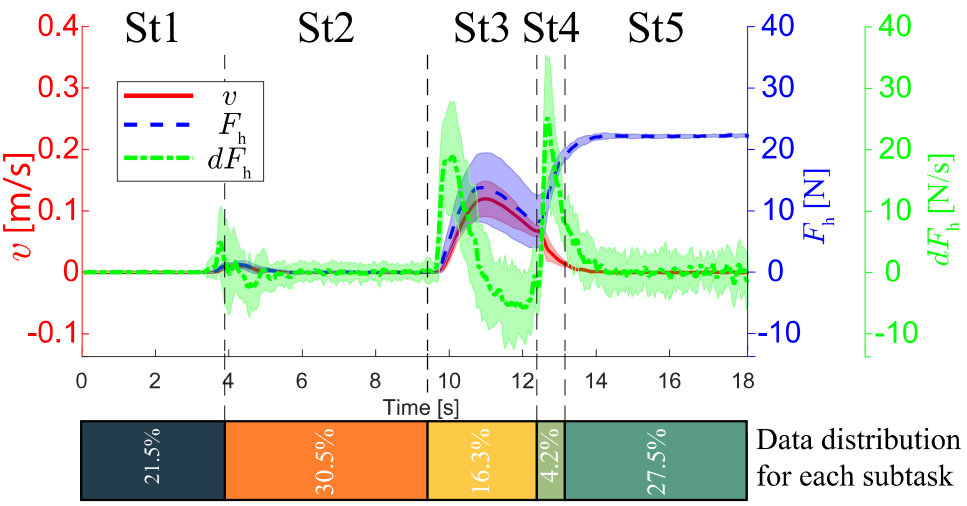

Figure 4.1: Mean and standard deviations of v, F_h, dF_h for all trials as functions of time, collected from a single subject. Percent distribution of data for each subtask is shown in the colored boxes.

4.1 The Case Against a Rule-Based Approach

An idea to design a rule-based approach for our pHRI task is to come up with subtask transition rules using the features, v, F_{h}, dF_{h}. This can be facilitated by using the means, of the respective features, v_i^{μ}, F_i^{μ}, dF_i^{μ} and standard deviations observed during example executions, where i stands for a subtask in a trial. We calculate these means for each subject, then plot the means of means and standard deviations of means for all subjects in Figure 4.2.

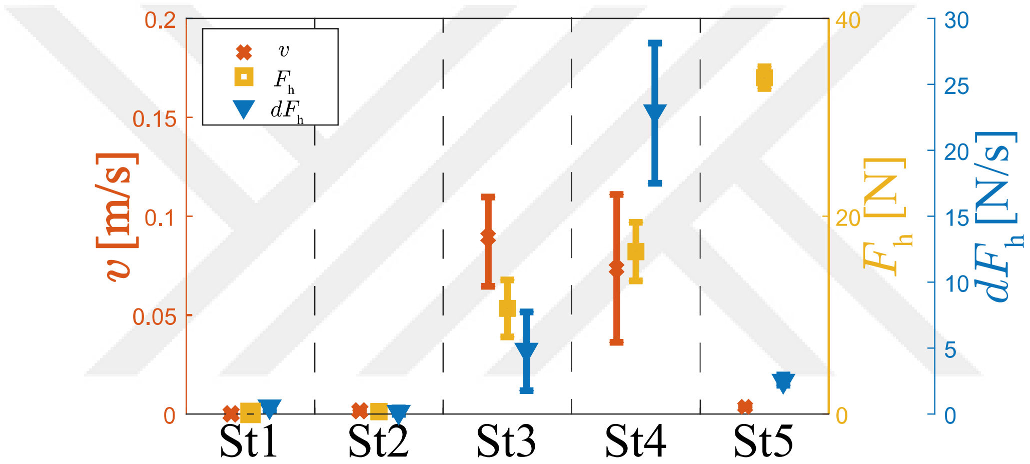

Figure 4.2: Mean of means of each metric and standard deviation of means for data of all subjects for each subtask.

These descriptive statistics depicted in Figure 4.2 show that there is no easy way to differentiate St1 and St2 from each other as all the mean values are very close to each other. Similarly, distinguishing St3 from St4 is only possible by utilizing dF_i^{μ}. However, St3 is closely related to how aggressive the human interacts with robot while executing the subtask, so derivative of force alone may not be sufficient in practice. On the other hand, St5 can be recognized by F_i^{μ}. However, a significant portion of F_h is used for compressing the spring. When a softer spring is present which requires less force, St5 may be confused with other subtasks using this rule. To sum, constructing a rule-based approach is not a straightforward procedure.

4.2 Evaluation of Our Machine Learning Approach

We first evaluate our models with a modified cross-validation approach. We train them with the data of 9 participants and testing with the remaining one, and rotate the tested participant. The resulting mean recognition accuracy is 96.5 (0.8)%. This shows that subtasks can be recognized with our approach in the given pHRI scenario with a high accuracy if there is a large amount of training data.

We then increase the difficulty of our evaluation by using another modified cross-validation approach. For this, we train our models with the data of only a single participant and use the data of remaining 9 for testing. The resulting mean recognition accuracy is still very high, considering the difficulty of the evaluation, 91.7 (2.2)%. This shows that our LSTM models can learn the essential structure of each subtask from a single subject. Also, a low standard deviation points out that our subtask recognition method is subject independent. Evaluations above show that the subtask recognition with deep learning is a viable idea.

Chapter 5

EXPERIMENT-II: ROBUSTNESS CHECK

Having shown the viability of subtask recognition, we consider possible conditions that can be encountered in pHRI (see Chapter 3). Our proposed method should be robust to those challenges for practical use.

In this experiment, 5 male subjects (median age: 30) participated and there were 5 different experimental conditions (EC, see Table 3.1) which were all displayed to each subject (S). For each EC, there were 6 sets of controller parameters similar to the previous experiment. There were 30 (5x6) trials for each condition and 150 (5x30) trials for each subject.

5.1 *Results and Discussion*

There were 25 (5x5) pairs of subject-experimental condition combinations (S/EC) in this experiment. We trained our model with data of an S/EC pair and test the model with data of the remaining pairs. There were 24 test sets for each model trained with a pair of S/EC. So, there were 600 (25x24) test accuracies. We present the mean values and standard deviations of these by averaging out the subjects in Table 5.1.

5.1.1 Verification of the results of Experiment-I

In each train-test combination, except where the models were trained with EC3 (shaded in red in Table 5.1), recognition accuracy was around 90%, which verifies the findings of Experiment-I, implying that subtask recognition is a viable idea despite different experimental conditions. Low standard deviations in recognition accuracies further support that subtask recognition with our approach is subject independent.

Table 5.1: Train-Test Sets of the Experiment-II: Mean Recognition Rates (Standard Deviations) %

		Train				
		EC1	EC2	EC3	EC4	EC5
Test	EC1	91.1 (1.2)%	91.6 (0.9)%	72.6 (5.8)%	91.6 (1.1)%	92.0 (1.3)%
	EC2	90.8 (1.4)%	91.3 (1.3)%	68.2 (2.9)%	90.8 (1.6)%	91.3 (1.5)%
	EC3	89.2 (1.1)%	89.8 (1.2)%	73.3 (5.9)%	88.3 (1.3)%	89.4 (1.3)%
	EC4	90.5 (1.1)%	90.8 (1.4)%	70.8 (4.8)%	91.1 (1.3)%	90.9 (1.7)%
	EC5	89.9 (1.1)%	90.7 (1.2)%	70.8 (5.0)%	90.0 (1.5)%	90.2 (1.7)%

5.1.2 Robustness to changes in human arm configuration

In EC4, subjects performed the task with a different human arm configuration (HAC2). Recognition accuracy for the cases where EC4 was included in either train or test sets was still around 90%. This provides evidence that our approach is robust to changes in human arm configurations.

5.1.3 Robustness to variations in controller parameters

A different set of controller parameters (CPS2) was used in EC5. When train or test set contained EC5, recognition accuracy was over 90%. Hence, we can argue that our method is robust to changes in controller parameters.

5.1.4 Robustness to changes in environmental stiffness

In EC2 and EC3, a lower and higher stiffness values of K_{low} and K_{high} were utilized. Table 5.1 shows that when EC2 was in either the training or the test sets, recognition accuracy was around 90%. Moreover, when the test set included EC3, recognition accuracy was still over 90%. However, when EC3 appeared in training set, recognition accuracy dropped to around 70%.

Table 5.2: Confusion Matrix where model is trained with data of S1/EC1 and tested with data of S2/EC2.

		Train				
		St1	St2	St3	St4	St5
Test	St1	2386	80	11	2	0
	St2	150	3256	7	2	0
	St3	27	192	1340	31	0
	St4	0	0	81	498	55
	St5	0	0	0	38	3120

Our results show that our method is robust to variations in task conditions that we mentioned before as all test accuracies were around 90% except the case where train set included EC3 (K_{high}/HAC1/CPS1). For instance, when we use the model trained with the data corresponds to EC1, we can still recognize the subtasks under other experimental conditions. Table 5.2 shows a confusion matrix of such a case where the model is trained with data of EC1 and tested with data of EC2. Investigating the confusion matrix reveals that the trained model recognizes each subtask with high accuracy but mismatches occur mostly at adjacent subtasks. Those mismatches may indicate that there may be a transitional subtask between two adjacent ones which we did not consider as we aimed to focus on the recognition of the salient subtasks. Moreover, the confusion matrix points out that the model can distinguish St1 from St2 which means that the model can sense whether the user grasps the handle or not.

As mentioned above, the cases which include EC3 in the training set result in lower test accuracy. Analyzing the confusion matrix that corresponds to such a case reveals that most of the misclassifications occur in the recognition of St5 (see Table 5.3). Models confuse St5 with St4 considerably.

Table 5.3: Confusion Matrix where model is trained with data of S3/EC3 and tested with data of S4/EC1.

		Train				
		St1	St2	St3	St4	St5
Test	St1	2374	138	30	37	0
	St2	160	3464	161	3	0
	St3	29	305	2042	17	0
	St4	0	0	134	512	5
	St5	0	0	4	3116	32

We investigated this issue by trying various approaches to tackle the drop in the recognition rates. For instance, we used different LSTM hyperparameters and more aggressive dropout rates which did not yield considerable improvements. We only managed to increase the recognition rates by two ways as reported below:

Training the model with combinations of data When models were trained using the data collected from all subjects under EC3 excluding the data of the subject in the test set, recognition accuracy increased up to 95%. So, we observed that, testing the models trained with EC3 does no longer yield low test accuracies. In particular, recognition accuracy increased to 94.5 (0.8)%, 94.8 (0.5)%, 92.7 (1.3)%, 94.2 (1.9)%, 94.3 (0.8)%, with test sets corresponds to EC1, EC2, EC3, EC4, EC5, respectively. This suggests that data size should be increased to improve recognition accuracy of models trained with data collected with stiffer environments (as in EC3).

- We can increase our test accuracy by training all the data collected from all users except the test user - (Predicting one subject's subtasks by training the model with data of the remaining subjects)

- We can increase our test accuracy by training all the data collected from single subject's data (Predicting one subject's subtasks by training the model with another subject's data)

Combining last two subtasks Due to the nature of contact, "contact" subtask (St4) is an event-like subtask where the duration of it is significantly smaller than that of other subtasks (see Figure 4.1). We believe that low test accuracies may be due to high capacity of the utilized deep learning method, LSTM. The trained models may have memorized the St4 in such a way that it mainly confuses the St5 with St4. As we discussed in Section 3.1, we were aware that the boundary between the last two subtasks (St4 and St5) may not be determined easily by expert supervision alone. For this reason, unsupervised segmentation techniques [25-30] can be exploited for determining subtasks which is not in the scope of this study. For the time being, as a remedy, we investigated combining the last two subtasks into a single one. As a result, the model trained with data corresponds to springs having high stiffness (as in EC3) no longer fails in predicting the new combined subtask. Test accuracies obtained after decreasing the number of subtasks are 91.3%(±5.4%), 92.0%(±1.8%), 90.9%(±2.1%), 86.7%(±7.3%), 88.6%(±7.5%), when the corresponding test sets are composed of EC1, EC2, EC3, EC4, EC5, respectively.

Chapter 6

EXPERIMENT-III: INTEGRATION OF SUBTASK RECOGNITION IN AN ADAPTIVE ADMITTANCE CONTROLLER

So far, we have verified that subtask recognition is a viable approach and robust against possible challenges that can be encountered in a pHRI task. For the next step, we implemented an adaptive admittance controller based on the proposed subtask recognition approach to investigate if recognition in real time is possible and such an adaptation approach can improve the task performance.

6.1 Experimental Procedure

In this experiment, we considered three different controllers and compared the task performance under each of them. The first controller, DL, is a variable admittance controller based on human intent prediction using Deep Learning. Here, the damping parameter is altered on-the-fly based on the executed subtask as we define human intent as the subtask being performed. In DL, the subtasks are recognized in real time based on our proposed subtask recognition approach. To this end, DL utilizes the LSTM model previously trained with the data collected from all the subjects participated in Experiment-I. The second controller, GT, named as the Ground Truth controller, is also a similarly structured variable admittance controller. In GT, subtasks are recognized using a specifically tuned algorithm for the considered pHRI task based on the position of the end-effector, which is essentially a rule-based approach. In other words, subtasks are already hardcoded in the system based on the end-effector position (rules given in Section 3.1.2 are used for the separation of subtasks). The last one, B, is a standard admittance controller used as a Baseline in the comparison where the controller parameters are fixed during the task. We selected controllers B and GT such that we can effectively compare DL with them. In adaptive controllers (GT and DL), only the damping parameter of the admittance controller is changed to keep the analysis of the experimental results more digestible (in this experiment, admittance mass value is set as 5 kg).

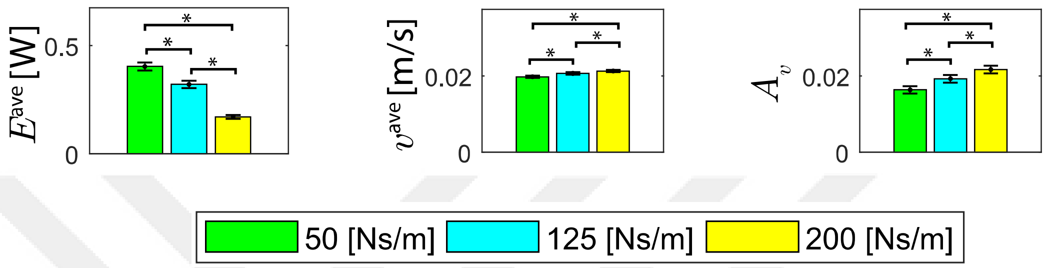

Figure 6.1: Means and standard errors of means of performance metrics calculated for Experiment I, see Section 6.2 for the definitions. Horizontal bars with * on top indicate statistically significant difference under the results of two corresponding damping.

Controller B is a standard admittance controller utilizing a constant mass and damping parameter. We use B as a baseline in the comparison with adaptive controllers. As the damping parameter, we selected one of the three available damping values utilized in Experiment-I (see Table 3.1). For the selection, we analyzed the task performance obtained in Experiment-I (see Figure 6.1) under each damping. We observed that average velocity under lower damping values was higher. We found that effort made by the participants reduced at the expense of an increase in oscillation amplitudes in velocity as the damping parameter decreased. Therefore, since the moderate damping value utilized in Experiment-I, b = 125 Ns/m, enables a compromise between improved effort and reduced oscillation amplitudes, it is selected as the constant damping parameter of controller B.

Table 6.1: Admittance Damping of Adaptive Controllers Associated to Each Subtask.

St1	St2	St3	St4	St5
200	125	50	200	125

In adaptive controllers, once the executed subtask is recognized, the admittance damping is altered on-the-fly according to preset damping values as shown in Table 6.1. Experts in pHRI have determined these values based on the following reasons.

At St1, as there is no physical contact between human partner and robot, robot is not desired to move. So, the damping value is set to the highest value in Table 6.1 to reject possible noise and external disturbances efficiently at this phase.

At St2, human partner grasps the handle attached to the robot. In a real scenario, this will signal that the execution of a pHRI task is about to begin. For this reason, a lower damping value is needed to start motion easily. However, much lower damping values would result in high jerk at the beginning while the human partner adjusts her/his arm impedance. So, a moderate damping value is selected (see Table 6.1).

At St3, we assume that human partner desires to move the robot with minimal effort, so the lowest available damping value is selected for this subtask.

At St4, the contact with the environment occurs suddenly while the damping is already set to a low value, combination of which threatens the stability of the coupled system most. In order to maintain stability robustly at this phase, we set the damping to the highest available value in Table 6.1.

At St5, as the participants try to park while compressing the spring, high damping value may help precise positioning. However, high damping may result in increased effort by the user. Moreover, the user may change her/his mind and move to another target location in a practical scenario which requires lower damping. So, in this subtask, the damping is set to the moderate value.

If a change in the subtask is detected, switching from the previous damping value to the desired damping of the current subtask occurs linearly in preset time duration. In preliminary experiments, 3 naive and 2 expert users tested this switching mechanism with various durations ranging from 16 ms to 500 ms. As users preferred 200 ms over the others, this value is used in this experiment.

We believe that, occasionally, experienced users will prefer lower damping in the admittance controller to reduce their effort. They, subconsciously, would calibrate their arm impedance so that stability of the robot will not be jeopardized. In order to make a fair comparison between the controllers considered in this experiment, subjects with no previously interaction experience with the robot were allowed to participate. 18 naive subjects (9 male, median age: 26.5) participated in this experiment. As there are three different controllers, possible permutations of these controllers yield 6 different sets. Each set was tested by 3 randomly selected participants, while those participants did not participate in sessions for other sets. A participant tested each controller 5 times in a row to get familiar with the setup. Then, in the data collection phase, each one executed the task 10 times under a given controller back to back. After every 10 trials corresponding to each controller, subjects were asked to complete a short questionnaire.

6.2 Performance Metrics

We use average velocity ($v^{\text{ave}} = 1/(t_e - t_b)\int_{t_b}^{t_e} |v|\, dt$) and average effort ($E^{\text{ave}} = 1/(t_e - t_b)\int_{t_b}^{t_e} |F_h v| dt$) to quantify the interaction performance under different controllers, where, t_b and t_e are the respective beginning and ending times of a subtask or a trial. In addition, amplitude of oscillations in velocity as a function of frequency is computed using FFT analysis and $A_v = 1/(\omega_U - \omega_L)\int_{\omega_L}^{\omega_U} v(\omega) d\omega$ for a range of frequencies is evaluated as a measure to compare the relative dissipation capacity under each controller, where $v(\omega)$ is the Fourier transform of $v(t)$, and ω_U and ω_L are the upper and lower bounds of the frequency range, respectively. The upper bound is selected as $\omega_U = 10$ Hz in light of Brooks et al. [25].

6.3 Data Analysis

For each subject, the performance metrics were calculated for entire duration of a trial. These metrics were also computed for individual subtasks to quantify the task performance at each subtask. We performed repeated measures one-way ANOVA to investigate the statistical significance of these results. In all statistical analyses, a significance level of $p = 0.05$ was used to test the null hypothesis.

6.4 Results and Discussion

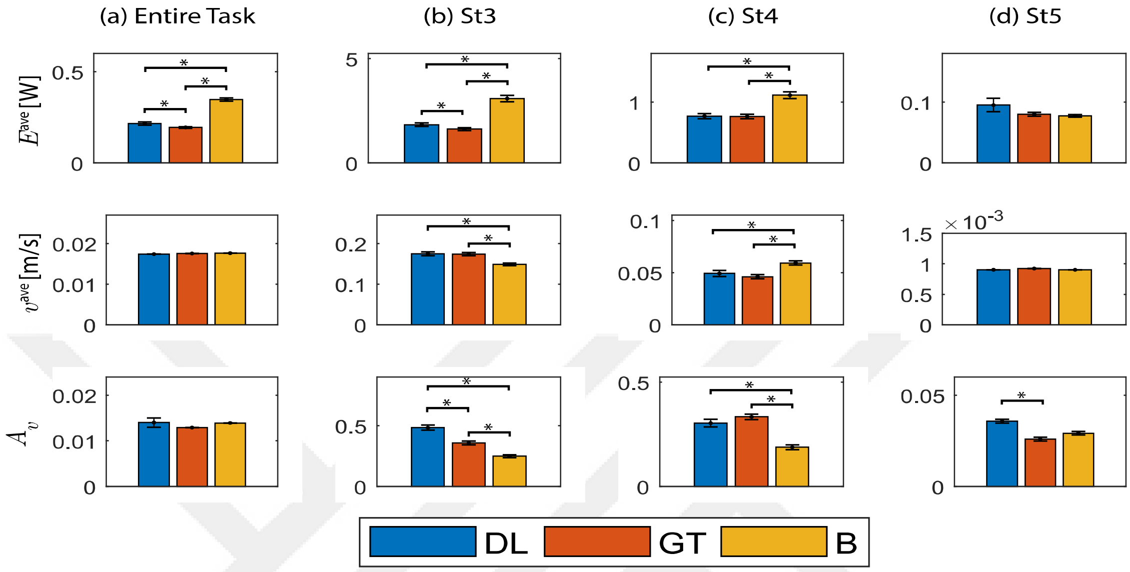

Figure 6.2: Means and standard errors of means of performance metrics calculated for both entire task and individual subtasks (St3, St4, and St5). Horizontal bars with * on top indicate statistically significant difference between the results of two corresponding controllers.

Figure 6.2-a shows that utilization of adaptive controllers (GT and DL) reduces effort considerably during the entire task. This shows that if subtask recognition can be performed in real time, and damping parameter of the admittance controllers are altered on-the-fly based on the subtask properly, effort by human can be reduced. On the other hand, effect of controllers on v^{ave} and A_v was not significant. The main reason is that the duration for holding the position during St5 dominates overall task. In particular, achieving similar velocities in all controllers enables fair comparison between the controllers in terms of effort since effort is highly depended on task duration and velocity.

In addition to inspecting the metrics during the entire task, we also evaluated them for each subtask to compare the effect of controllers on these metrics at each subtask. Although St1 and St2 was considerable parts of the task, we divided the subtasks into two groups; non-active subtasks (St1-St2) and active subtasks (St3-

St4-St5) to see the effect of the adaptive controller on the active subtasks. Since St1 and St2 involve no intentional movements, there is no need to inspect neither effort nor velocity. Therefore, we only examined these metrics during St3-St4-St5.

Performance metrics during St3 is illustrated in Figure 6.2-b. We observed that E^{ave} under the adaptive controllers (GT and DL) are significantly lower than that of controller B. In addition, v^{ave} under B is lower than the adaptive controllers as the participants may prefer to move with lower velocity under this controller, due to the high effort.

Figure 6.2-c depicts the performance metrics during St4. We observed that E^{ave} under adaptive controllers were significantly lower than that of B. However, A_v under B was significantly lower than that of others. Controller B utilizes a fixed damping throughout the task wehereas the damping was increased over time in adaptive controllers during St4. Note that changing the damping adaptively is a disturbance to the system in essence. So, higher amplitude oscillations are expected under adaptive controllers. Though, such increased amplitudes should not jeopardize the stability of the interaction. Note that no instability was observed under any controllers tested.

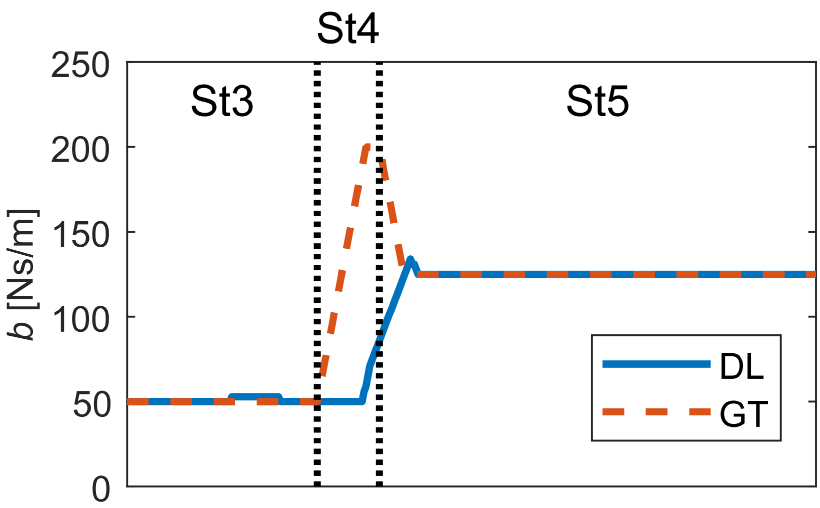

Figure 6.3: Damping profiles under GT and DL from the corresponding trials of a subject during St3, St4, and St5.

In Figure 6.3, damping profiles collected from a single subject are illustrated. Controller GT detects the beginning of St4 as soon as a specific position is achieved due to its specific tuning, disregarding the actual human intent. On the other hand, DL seems to capture St4 slightly later than GT, and damping switch is triggered after a while under DL. However, please note that DL considers the human intent. As subjects may continue to their movement even in the beginning of contact, DL continues to render lower damping as it assumes that St3 is continued. This shows a potential advantage of DL over GT as DL is designed to comply with human intent.

The performance metrics evaluated for St5 are shown in Figure 6.2-d. Inspecting this, we observed that A_v under B was lower than that of DL. Moreover, the lowest A_v was achieved under GT. GT renders the highest damping at St4, regardless of the human intention. That's why movement under GT is already highly damped before St5 begins. So, the lowest A_v under GT is expected. On the other hand, damping may not reach to the highest value before St5 begins under DL. That's why higher A_v can be expected under DL.

Considering the results mentioned above, it is clear that not only adaptive controllers outperform the baseline one B, but also the controller DL utilizing the proposed subtask recognition approach performs similarly to GT. DL considers human intent while subtask recognition of GT utilizes a task specific manually tuned approach. The definitions of subtasks for the experimental scenario are hardcoded in GT disregarding the human intent. However, we can argue that such an approach cannot be used for other tasks as even a slight change in the target location degrades the reliability of GT significantly. On the other hand, DL considers the human intent and does not use any task specific information (i.e., position) while it still performs very similarly to GT. Please note that we do not expect DL to outperform GT, but DL performing in a very similar performance with GT in ideal working condition of GT is more than sufficient to show the superiority of DL. Unlike GT which is a rule-based approach specifically tuned for a particular task, DL does not require fine-tuning for different conditions, and moreover, subtask recognition approach of DL can also work for complex pHRI tasks. Considering these, we can easily conclude that not only the proposed approach can recognize subtasks in real time successfully, but also utilizing an adaptive controller (i.e., DL) based on this approach is more desirable as it results in increased task performance while not requiring much effort to implement.

As the quantitative results presented above show the benefits of DL over GT, we further evaluated the controllers qualitatively. During the experiments, we requested the participants to complete a questionnaire. In the questionnaire, we asked the participants to compare the control techniques in terms of (1) sense of collaboration, (2) comfortableness, (3) trustworthiness, (4) level of enjoy, and (5) preference. We did not find any effect of controllers on responses of subjects. So, this implies that using controller DL results in a significant improvement in task performance while it does not cause any considerable negative feeling on the participants.

Chapter 7

DISCUSSION

In this study, we hypothesize that pHRI tasks can be defined as a collection of subtasks. When these subtasks are recognized in real time, appropiate controller or controller parameters can be used to improve task performance.

In the literature, most of the researchers define human intent as a low-level concept, like intention to accelerate/decelerate using features such as instantaneous velocity/force. Once human intention is estimated using such approaches, how to make use of those estimated intentions is not clear. Novelty of this work is that we consider human intention as a high-level concept. We show that when subtask is recognized as human intent, adaptive controllers can comply with the requirements of that specific subtask contributing to the improvements in overall task performance. As a result, our approach yields to a more feasible solution.

In our study, we compare standard admittance controller with adaptive ones. We show that adaptive controllers based on subtask recognition result in an improved task performance compared to standard controllers. The main difference between the two adaptive controllers (DL and GT) considered in this study is the way how the subtasks are recognized by them. DL utilizes a deep learning technique (LSTM) to recognize the subtaks by considering the intent of the human operator. On the other hand, GT relies on a subtask recognition approach which is task specific (i.e., position dependent), disregarding the intention of the human completely. Supported with both quantitative and qualitative results, we show that DL performs similarly to GT, while GT is tested under its ideal working conditions (note that GT was specifically tuned for the pHRI task considered during experiments). A slight change in the task conditions would make GT useless. On the other hand, DL would outperform GT as DL will perform robustly to much more challenging pHRI conditions. Note that DL takes advantage of the subtask recognition approach using LSTM which was shown to perform robustly against various challenging pHRI conditions (see Chapter 5). While doing so, the LSTM model adopted by controller DL does not rely on any task specific information while predicting the human intent. Therefore, we offer to use ML to leverage our subtask recognition approach which is well-suited for applications that involve pHRI.

In this study, we claim that there are universal subtasks which are common in various physical collaborative tasks. Even though, we only handle five of them within the scope of this study, one can prepare a larger set of universal subtasks considering many other pHRI tasks. Once such a universal set of subtasks are defined, the required actions can be taken by the controllers to meet the requirements of the recognized subtasks. For instance, a controller having higher damping capacity is needed to allow precise movements when universal subtasks require high precision. Our approach could be easily adopted to recognize a larger set of universal subtasks, so this would bring more flexibility in designing task-independent adaptive controllers. Therefore, systems can be set up with less investment and less labor force.

Throughout this study, we focused on a 1-D task to increase the controllability over experimental conditions (especially in Experiment II and Experiment III, see Chapters 5 and 6) and keep the tractability and digestibility of the results. For instance, in the second experiment, we challenged our approach by asking participants to move strictly in longitudinal or transverse directions around two different human arm configurations, HAC1, and HAC2, respectively (see Figure 3.3). In a multi-dimensional setup, it would be harder to constrain participants to maintain their arm configurations, so results would lose their tractability. Also, for the third experiment, we ran statistical analyses over performance metrics for three different control techniques. For this purpose in a multi-dimensional task, the experimental setup should be prepared with more caution since subjects could perform unforeseen actions, considerably affecting the results. Thus, interpretation of the findings would be more difficult. Despite all these, we want to highlight that it is not difficult to extend our subtask recognition method for a multi-dimensional system, as we foresee no restriction to do so.

Chapter 8

CONCLUSION AND FUTURE WORK

In this work, we highlight the idea that many tasks of interest are made of sequential subtasks and define human intention as the current subtask to be executed. These subtasks have different requirements (e.g. moving to a location vs precise positioning) and require different robot behaviors to be executed efficiently. If the robot can recognize the subtask that the human is intending to execute in real time, it can adapt itself. Motivated by this, we put forth the idea of subtask recognition using a time-window of measured robot velocity, applied human force and its derivative during the interaction. We formulated this as a time series prediction problem and proposed a deep learning approach to solve it.

To test our approach, we performed three pHRI experiments involving a 1-D abstraction of a drilling task. The initial experiment showed that our approach can achieve high recognition rates ($> 90\%$) even when trained with the data of a single participant and tested on the rest. This verifies that subtask recognition is viable with our approach and that it is robust to changes in the human operator. Based on these results, the second experiment was designed to test the robustness of our approach in more challenging conditions. In addition to verifying the first experiment, the second experiment showed that our approach to subtask recognition is robust to changes in human arm configuration, controller parameters, and environment stiffness achieving around 90% accuracies for most robustness tests. We further showed that the low accuracy cases can be alleviated with more data. In the third experiment, we showed that subtasks can be recognized in real time utilizing our approach, and an adaptive admittance controller based on subtask recognition can enhance the task performance while not interfering with the user's perception. In particular, we showed that adaptive controllers based on human intent are superior than baseline controllers since it adapts itself to comply with the user's intent.

In our research, we considered that a collaborative task consists of several salient subtasks which are typically common in many tasks. However, we believe that there could be some transitional subtasks as well as task specific ones. From this perspective, dividing a collaborative pHRI task into subtasks is still an open question.

An immediate research direction that our work can take can be following. In most manufacturing environments, processes have well-defined recipes where labeling of subtasks for supervised learning could be feasible. However, there could be cases where this is not practical. An interesting avenue for future research is employing unsupervised time series segmentation to divide such tasks into subtasks. On the other hand, in this work, we assumed that the appropriate controller parameters for each subtask were known a priori. However, selecting a suitable damping parameters for each subtask is also an open research problem that we aim to tackle in the future. To this end, another interesting research direction could be altering controller parameters on-the-fly depending on the performance requirements of each subtask. Techniques based on reinforcement learning (RL) can be used to find appropriate policies to better address such requirements.

BIBLIOGRAPHY

[1] D. P. Losey, C. G. McDonald, E. Battaglia, and M. K. O'Malley, "A review of intent detection, arbitration, and communication aspects of shared control for physical human–robot interaction," *Appl. Mechanics Rev.*, vol. 70, no. 1, p. 010804, 2018.

[2] N. Hogan, "Impedance control: An approach to manipulation," in *American Cont. Conf.*, 1984, pp. 304–313.

[3] A. Q. Keemink, H. van der Kooij, and A. H. Stienen, "Admittance control for physical human–robot interaction," *The International Journal of Robotics Research*, vol. 37, no. 11, pp. 1421–1444, 2018.

[4] N. Stefanov, A. Peer, and M. Buss, "Role determination in human-human interaction," in *IEEE World Haptics Conf.*, 2009, pp. 51–56.

[5] A. Mortl, M. Lawitzky, A. Kucukyilmaz, M. Sezgin, C. Basdogan, and S. Hirche, "The role of roles: Physical cooperation between humans and robots," *Int. J. Robot. Res.*, vol. 31, no. 13, pp. 1656–1674, 2012.

[6] S. O. Oguz, A. Kucukyilmaz, T. M. Sezgin, and C. Basdogan, "Supporting negotiation behavior with haptics-enabled human-computer interfaces," *IEEE Transactions on Haptics*, vol. 5, no. 3, pp. 274–284, Third 2012.

[7] A. Kucukyilmaz, T. M. Sezgin, and C. Basdogan, "Intention recognition for dynamic role exchange in haptic collaboration," *IEEE Transactions on Haptics*, vol. 6, no. 1, pp. 58–68, First 2013.

[8] J. R. Medina, M. Lawitzky, A. Molin, and S. Hirche, "Dynamic strategy selection for physical robotic assistance in partially known tasks," in *2013 IEEE*

International Conference on Robotics and Automation, May 2013, pp. 1180–1186.

[9] R. Ikeura and H. Inooka, "Variable impedance control of a robot for cooperation with a human," in *Proceedings of 1995 IEEE International Conference on Robotics and Automation*, vol. 3, May 1995, pp. 3097–3102 vol.3.

[10] V. Duchaine and C. M. Gosselin, "General model of human-robot cooperation using a novel velocity based variable impedance control," in *IEEE World Haptics Conf.*, 2007, pp. 446–451.

[11] Y. Aydin, N. Arghavani, and C. Basdogan, "A new control architecture for physical human-robot interaction based on haptic communication," in *ACM/IEEE Int. Conf. Human-Robot Interaction*, 2014, pp. 122–123.

[12] A. Lecours, B. Mayer-St-Onge, and C. Gosselin, "Variable admittance control of a four-degree-of-freedom intelligent assist device," in *2012 IEEE Int. Conf. on Robotics and Automation*, May 2012, pp. 3903–3908.

[13] T. Tsumugiwa, R. Yokogawa, and K. Hara, "Variable impedance control based on estimation of human arm stiffness for human-robot cooperative calligraphic task," in *IEEE Int. Conf. Robot. Automat.*, vol. 1, 2002, pp. 644–650.

[14] S. Grafakos, F. Dimeas, and N. Aspragathos, "Variable admittance control in phri using emg-based arm muscles co-activation," in *IEEE Int. Conf. on Syst., Man, and Cybern.*, 2016, pp. 1900–1905.

[15] L. Rozo, J. Silvério, S. Calinon, and D. G. Caldwell, "Learning controllers for reactive and proactive behaviors in human–robot collaboration," *Frontiers in Robot. and AI*, vol. 3, p. 30, 2016.

[16] F. Dimeas and N. Aspragathos, "Reinforcement learning of variable admittance control for human-robot co-manipulation," in *IEEE/RSJ Int. Conf. Intell. Robots Syst.*, 2015.

[17] E. C. Townsend, E. A. Mielke, D. Wingate, and M. D. Killpack, "Estimating human intent for physical human-robot co-manipulation," *CoRR*, vol. abs/1705.10851, 2017.

[18] P. Evrard, E. Gribovskaya, S. Calinon, A. Billard, and A. Kheddar, "Teaching physical collaborative tasks: object-lifting case study with a humanoid," in *IEEE Int. Conf. Humanoid Robots*, 2009, pp. 399–404.

[19] Z. Wang, A. Peer, and M. Buss, "An hmm approach to realistic haptic human-robot interaction," in *World Haptics - 3rd Joint EuroHaptics Conf. and Symp. on Haptic Interfaces for Virtual Environment and Teleoperator Systems*, 2009, pp. 374–379.

[20] I. Ranatunga, S. Cremer, D. O. Popa, and F. L. Lewis, "Intent aware adaptive admittance control for physical human-robot interaction," in *IEEE Int. Conf. Robot. Automat.*, 2015, pp. 5635–5640.

[21] S. Ikemoto, H. B. Amor, T. Minato, B. Jung, and H. Ishiguro, "Physical human-robot interaction: Mutual learning and adaptation," *IEEE Robot. & Automat. Mag.*, vol. 19, no. 4, pp. 24–35, 2012.

[22] T. Tsuji, P. G. Morasso, K. Goto, and K. Ito, "Human hand impedance characteristics during maintained posture," *Biol. Cybern.*, vol. 72, no. 6, pp. 475–485, 1995.

[23] Y. Aydin, O. Tokatli, V. Patoglu, and C. Basdogan, "Fractional order admittance control for physical human-robot interaction," in *IEEE World Haptics Conf.*, 2017, pp. 257–262.

[24] ——, "Stable physical human-robot interaction using fractional order admittance control," *IEEE Transactions on Haptics*, 2018.

[25] T. L. Brooks, "Telerobotic response requirements," in *IEEE International Conference on Systems, Man, and Cybernetics Conference*, Nov 1990, pp. 113–120.